Anion–Protein Interactions during Halorhodopsin Pumping: Halide Binding at the Protonated Schiff Base†

Timothy J. Walter and Mark S. Braiman*

Department of Biochemistry, University of Virginia Health Sciences Center, Charlottesville, Virginia 22908

Received August 12, 1993; Revised Manuscript Received December 1, 1993®

ABSTRACT: Halorhodopsin (hR), the light-driven chloride pump of *Halobacterium halobium*, has been studied by Fourier transform infrared (FTIR) spectroscopy. Direct hydrogen bonding of halide ions with the protonated Schiff base (PSB) group was detected by means of halide-dependent perturbations on this group's vibrational frequencies. FTIR difference spectra were obtained of the hR → hL photoreaction in reconstituted membrane vesicles. Nearly identical results were obtained using either low-temperature static difference spectroscopy at 1-cm^{-1} resolution or a stroboscopic time-resolved technique with 5-ms temporal and 2-cm^{-1} spectral resolution. The frequency of the negative difference band due to the PSB C=N stretch mode in the hR state shows a dependence on the type of halide counteranion that is present, 1632 cm^{-1} in the presence of Cl^-, 1631 cm^{-1} in Br^-, and 1629 cm^{-1} in I^-. The C=NH^+ stretch frequency thus correlates with the strength of the hydrogen bond formed by the halide. Analogous halide-dependent shifts of the C=NH^+ frequency were observed in IR spectra of model compound retinylidene PSB salts. We also observed a significant halide dependence of the visible absorption maximum of hR solubilized in lauryl maltoside detergent. From such halide perturbation effects, we conclude that there is a direct hydrogen-bonded interaction between the Schiff base group and an externally supplied halide ion in the hR state. Halide perturbation effects are also observed for PSB-group vibrations in the hL state. Thus, despite an apparent overall weakening of hydrogen-bonding interactions of the PSB with its environment after chromophore photoisomerization to form hL, the PSB remains hydrogen-bonded to the halide. The results are best explained in terms of a "one-site, two-state" model for anion binding near the chromophore in the hR state, as opposed to a previously proposed two-site model.

Halorhodopsin (hR, MW 27 000)[1] is an integral membrane protein of the *Halobacterium halobium* cell envelope which has been shown to function as an electrogenic light-driven chloride pump (for a review, see Lanyi, 1990). It bears ~30% amino acid sequence identity with the well-studied proton pump bacteriorhodopsin (bR). It also exhibits many of the same overall structural features, including: seven transmembrane α-helical spans, an *all-trans*-retinal chromophore which photoisomerizes to 13-*cis* in the initial photochemical event, and a protonated Schiff base (PSB) linkage between the terminal carbon of the chromophore and a lysine residue in the seventh transmembrane helix.

Despite these structural similarities, the photochemical reactions of hR and bR differ significantly, at least under physiological conditions (Oesterhelt & Tittor, 1989). The hR photocycle lacks any intermediate analogous to the M state of the bR photocycle. This 410-nm absorbing species is the only bR photointermediate with a deprotonated Schiff base. Its absence from the hR photocycle means that the Schiff base in hR represents a positive charge maintained with the bilayer at all stages of the photocycle. It is likely that hR forms no M-like intermediate because it lacks an internal anion homologous to the bR residue Asp-85. This residue serves as the proton acceptor from the chromophore PSB when M is formed from bR (Braiman et al., 1988). It has been proposed that an external Cl^- ion binds to hR in place of Asp-85 in bR (Diller et al., 1987; Dér et al., 1991; Ames et al., 1992). External anions binding at or near this site would be expected to affect a variety of biochemical and biophysical properties, including the visible absorption maximum of the retinal chromophore, the pK_a of its Schiff base group, and the vibrational frequencies of the -C=NH^+ moiety as well as the shifts observed for these vibrations upon deuteration of the PSB.

The aforementioned properties are listed in order of increasing specificity in providing information about hydrogen-bonding interactions of the counterion with the Schiff base. For example, the visible absorption maximum would be shifted by anions binding at the Schiff base and also at other sites in the retinal binding pocket. Indeed, this has been invoked in the previously proposed two-site model for anion binding to hR (Schobert et al., 1986; Lanyi et al., 1988). In this model, occupancy of the site near the Schiff base by a (non-halide) anion shifts the visible λ_{max} to the blue, while occupancy of a second (halide) anion at another location within the binding pocket shifts λ_{max} to the red. Likewise, the 1.5-unit increase in the pK_a of the hR Schiff base in the presence of halides, nitrate, and several other inorganic anions (Schobert et al., 1986) is probably indicative of closer interactions between these external anions and the PSB but still does not necessarily imply direct binding to the PSB because of the potentially long range over which electrostatic forces can act in the low-dielectric environment of the membrane. The vibrational modes of the C=NH^+ moiety, however, are expected to be perturbed more specifically by short-range interactions such as direct hydrogen bonding with the Schiff base (Fodor et al., 1987; Ames et al., 1992) or π-orbital overlap between the

† Supported by NIH Grant GM46851. T.J.W. is a Howard Hughes Medical Institute Predoctoral Fellow.

* Address correspondence to this author.

® Abstract published in *Advance ACS Abstracts,* February 1, 1994.

[1] Abbreviations: hR, halorhodopsin; bR, bacteriorhodopsin; o.g., β-D-octylglucoside; TR, time-resolved; FTIR, Fourier transform infrared; PSB, protonated Schiff base; NRBA, *N*-retinylidene-*n*-butylammonium.

0006-2960/94/0433-1724$04.50/0

anion and the Schiff base nitrogen (Maeda et al., 1985). These vibrations thus serve as the most explicit indicator of the Schiff base environment.

The most sensitive differentiation between hydrogen-bonded and non-hydrogen-bonded charged groups in the vicinity of the Schiff base generally requires measurement of both C=NH and C=ND frequencies of the PSB group. Perturbation by non-hydrogen-bonded charges leads to near-equal shifts of both frequencies; whereas hydrogen bonding affects the C=NH frequency more than the C=ND frequency (Baasov et al., 1987). Thus, generally speaking, the single most explicit indicator of the strength of hydrogen-bonding interactions of the PSB group with its surroundings is the deuteration-induced frequency shift of the C=N vibration.

Most evidence provided to date by vibrational spectroscopy has favored the view of a weak and indirect interaction, as opposed to direct hydrogen bonding, between the anion and the PSB in hR. Resonance Raman work (Maeda et al., 1985; Smith et al., 1984) showed that the Schiff base $C{=}NH^+$ stretching frequency in hR in unusually low and its deuterium shift small, indicating even weaker hydrogen bonding between the PSB and its environment in hR than in bR, which is already more weakly hydrogen-bonded than model compound chloride salts of retinal PSB (Kakitani et al., 1983). Furthermore, resonance Raman measurements of hR in buffers containing Cl^- or Br^- did not detect any dependence of the $C{=}NH^+$ stretch frequency on which halide was present (Pande et al., 1989). These data tended to disfavor the idea of a direct hydrogen-bonding interaction between halides and the PSB and were used to support a revised two-site model for anion interactions with the chromophore (Lanyi et al., 1990). In this model, complex anions such as nitrate bind within a few angstroms of the PSB (site I); simple halides bind instead at a distinct site (site II) that is too distant from the Schiff base to permit any hydrogen-bonding interaction.

The results presented herein call into question these earlier conclusions. In contrast to the resonance Raman data mentioned above, our FTIR difference spectra of the hR → hL photoreaction show a distinct downshift of the $C{=}NH^+$ stretching band in the hR state as the halide ionic radius increases from Cl^- to Br^- to I^-. These data demonstrate that there is a direct hydrogen-bonding interaction between the Schiff base and halide in the hR state. Band fitting indicates that there is a similar counterion dependence for the hL (positive) difference bands of the same spectra. This indicates that a halide–Schiff base H-bonding interaction is retained upon conversion of hR to hL. The results directly support a model in which photoisomerization of the chromophore translocates the halide ion, bound to the PSB group, from one location in hR to another in hL, as proposed previously by Ames et al. (1992).

EXPERIMENTAL PROCEDURE

Protein Purification and Reconstitution. Halorhodopsin was expressed in *H. halobium* strain L33, generously provided by Dr. Richard Needleman. This strain has the bR gene (*bop*) rendered nonfunctional by a transposon insertion (Ni et al., 1990) and the hR gene (*hop*) placed under the control of the *bop* promoter. Cells were grown under room lighting in a standard halobacterial growth medium (Braiman & Mathies, 1980), except that Inolex peptone was substituted by a different gelatin hydrolysate (Sigma). Cells were incubated at 37 °C in carboys—typically four at a time, each containing 4 L of media. Aeration (1–5 L/min in each 4-L carboy) was accomplished by using a small air compressor and a cylindrical gas-diffusion stone. A 5–6-day period of aerobic growth was followed by 1–2 days of growth without aeration. During the latter period, cell density remained at saturation, while the hR yield appeared to increase somewhat.

Extraction of hR from the cell pellet and subsequent purification relied on its solubilization by the detergents sodium cholate and o.g. (β-D-octylglucoside) and followed, with minor modifications, a method developed previously (Duschl et al., 1988). Cells from 16 L of growth media were lysed by osmotic shock and then the membranes were pelleted, washed twice with water, and resuspended in 20 mL of 4 M NaCl and 25 mM Tris, pH 7.2. To this membrane suspension was added 10 mL of 20% (w/v) sodium cholate, previously titrated to neutral pH. The mixture was stirred in the dark at room temperature for 30 min and then centrifuged (50000*g*, 1 h) to remove cholate-insoluble material.

The ~30-mL supernatant, containing cholate-solubilized lipids and protein, was loaded onto a 1- × 15-cm column of Phenylsepharose (Pharmacia) that had been equilibrated previously with a dilute cholate buffer (4 M NaCl, 0.4% sodium cholate, and 25 mM Tris, pH 7.2). Most of the yellowish cytochrome impurities eluted in the void volume, while the hR remained bound to the column. Elution of hR was with a linear gradient of o.g. (0.1–0.5% in 4 M NaCl and 25 mM Tris, pH 7.2), applied over 20 column volumes. This gradient elution scheme, which was not used by Duschl and Lanyi (1988), was found to be necessary to eliminate a 400-nm absorbing impurity from the pooled fractions and to produce hR with an A_{280}/A_{570} ratio of ~2. Typical yield was 20 mg of purified hR from 16 L of saturated L33 culture.

For UV/vis spectroscopy, the lipid-free hR in the column elution buffer was dialyzed for 48 h against 3 M KF, KCl, or KBr to remove o.g. The resulting aggregated protein was pelleted at 3000*g* and then resolubilized in the same 3 M salt solution containing 0.2% lauryl maltoside and 25 mM Tris, pH 6.5.

For all FTIR measurements, the hR from the column was reconstituted into native *H. halobium* polar lipids. These were obtained by extracting the washed membrane fraction of a separate portion of L33 *H. halobium* using the Bligh–Dyer (chloroform/methanol) extraction procedure (Bligh & Dyer, 1959) and then precipitating the lipids from chloroform solution with cold acetone supplemented with 0.01% $MgCl_2$ (Kates et al., 1982). The lipid:protein ratio in the reconstituted vesicles was in all cases near 5:1 (w/w). Special effort was made to insure that this ratio was identical among the samples to be examined for small halide-dependent spectral changes. To this end, column-purified hR (in a buffer containing ~3% o.g., 4 M NaCl, and 25 mM Tris, pH 7.2) was mixed with a 5 times greater amount of polar lipid (by weight) that had been sonciated in an equal volume of the same detergent buffer used for the hR. The mixture was only then divided into samples that were dialysed separately against 3 M KCl, KBr, or KI. The vesicles that formed upon removal of the detergent were pelleted and resuspended in 0.2 M KCl, KBr, or KI, containing also 25 mM Tris base with pH (or pD, for deuterated samples) adjusted to 7.2 using the appropriate hydrogen halide (or deuterium halide, obtained from Cambridge Isotope Labs.)

The reconstituted hR vesicles were repelleted and then a ~1-mg portion was transferred to a CaF_2 window and partially dried using a gentle stream of N_2. In the case of deuterated samples, this procedure was carried out in a glovebox saturated with ^2H_2O vapor. Each sample was squeezed to a thickness of ~10 μm with a second CaF_2 window, which had been

coated around its perimeter with a thin layer of vacuum grease to seal the sample.

Low-Temperature FTIR Spectroscopy. Difference spectra of the hR → hL photoreaction at 250 K were obtained using methods reported previously (Rothschild et al., 1988; Chen & Braiman, 1991). Briefly, the sample, sandwiched between two CaF_2 windows as described above, was mounted in a HeliTran cryostat (APD Cryogenics, Allentown, PA). The temperature was measured by a silicon diode and maintained at 250.0 K by a temperature controller (Scientific Instruments Model 9650).

All FTIR measurements were made on a Nicolet 60SXR spectrometer (Madison, WI). Steady-state conversion of hR to the hL photointermediate was accomplished by illuminating with 600-nm light for 15 min, during which time 250 interferograms were collected. The thermal reversal of hL back to hR was completed photochemically by 15 min of blue illumination ($\lambda \simeq 450$ nm), after which time the light was turned off and 250 more interferograms were collected. Fourier transforming each of these 16128-point interferograms yielded spectra at 1-cm^{-1} resolution. Ratioing successive light-on/light-off spectral pairs yielded absorbance difference spectra in which positive bands correspond to the hL photointermediate and negative bands correspond to the hR ground state.

Stroboscopic Time-Resolved Difference Spectra. Time-resolved FTIR spectra were obtained using a stroboscopic method applied previously to bR (Braiman et al., 1991). Reconstituted hR was sandwiched between CaF_2 windows as described above, and the windows were mounted in a water-bath-cooled holder maintained at 20 °C. The photocycle was initiated by a 30 mJ cm^{-2} flash at 532 nm from a frequency-doubled Nd^+-YAG laser (Spectra Physics GCR3). Timing of the flash and data collection were controlled by a modified version of the Nicolet 60SX time-resolved software. Time-resolved difference interferograms were collected stroboscopically, i.e., by combining interfergram points collected during different mirror scans to cover the range of retardation values needed for the desired spectral resolution. Difference interferogram points were sorted in groups of 16 (Braiman et al., 1991) or 512 (Braiman et al., 1987). These data groupings corresponded to temporal intervals of 0.24 or 5.0 ms, respectively. (These intervals are not in the exact ratio 16:512 due to use of somewhat different mirror velocities for the two different time resolutions.) See the figure legends for additional details.

RESULTS

Counterion Dependence of C=C and C=N Stretching Frequencies in hR and hL. Figure 1 shows spectra of the hR → hL photoreaction at 250 K in the presence of three different halide ions. These spectra, taken at 1-cm^{-1} resolution, all generally duplicate the features of hR → hL difference spectra taken earlier at 2-cm^{-1} resolution (Rothschild et al., 1988). However, a significant counterion dependence is observed for two negative (hR) difference bands in the 1650–1500-cm^{-1} spectral region, assignable to the $C{=}NH^+$ stretch and the ethylenic C=C stretch of the chromophore. The observed frequency of both bands was highest in the presence of Cl^-, at 1632 and 1523 cm^{-1}, respectively (see Figure 1A and Table 1). Substitution of Cl^- by Br^- lowers C=N and C=C stretching frequencies 1 cm^{-1} each and by I^- an additional 2–3 cm^{-1} each.

For the hL state (Figure 1A, positive bands), the local maximum of the C=C peak is at 1555 cm^{-1} and not perceptibly

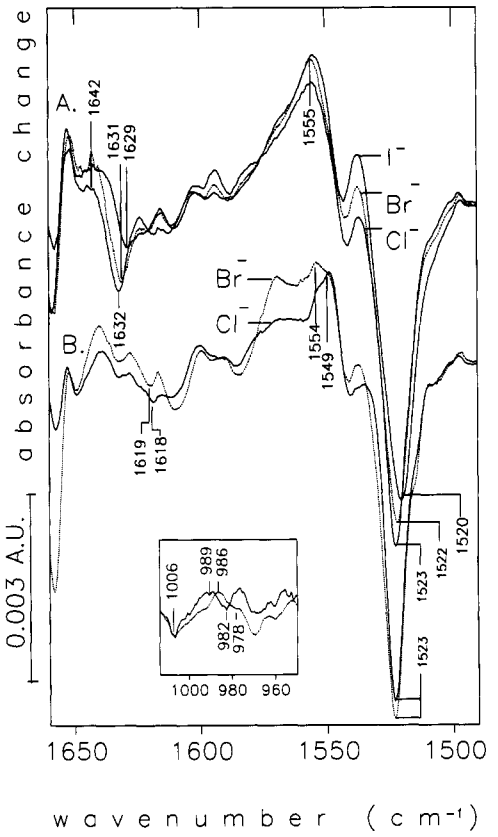

FIGURE 1: Halide dependence of the C=N and C=C stretching region of the hR → hL FTIR difference spectrum measured at 250 K. Positive bands correspond to the hL state and negative bands to hR. The *y*-axis scale is approximate; spectra were scaled relative to each other (by a factor of 4 at most) to give similar peak heights. Samples contained saturating concentrations of the potassium salt of the indicated halide in H_2O (A) or D_2O (B) at pH (or pD) 7.2. The lipid:protein ratio was approximately 5:1 (w/w) and was identical among the three samples in A and the two in B. Cl^- and I^- spectra are shown with solid lines, while Br^- spectra are shown with dotted lines. The inset shows the halide dependence of the C=N—D bending region of B, at the same *y*-scale as the main plot.

Table 1: Fitted Center Frequencies for Bands in the 1650–1620-cm^{-1} Region of the hR → hL Difference Spectra[a]

halide	band I (+)	band II (+)	band III (−)
Cl^-	1651.7	1642.3	1632.5
Br^-	1651.3	1641.7	1631.4
I^-	1652.2	1638.6	1629.4

[a] Based on the data shown in Figure 1A. All values are in units of cm^{-1}. Gaussian bandwidths were fitted initially along with peak positions. For each band, the optimal fitted bandwidth values obtained for the three different anions were within 10% of each other. Therefore, for the final fit to obtain center frequencies, bandwidths were constrained to the following values: band I, 4.55; band II, 7.50; and band III, 9.42. The estimated error for these frequencies is ~0.2 cm^{-1} for band III and ~0.5 cm^{-1} for bands I and II because of larger base-line reproducibility errors related to the intense background absorption near 1655 cm^{-1} (due to water and amide I vibrations).

dependent on the counterion. The C=N frequency (in Cl^-) has been reported in Raman spectra variously to be at 1644 cm^{-1} (Fodor et al., 1987) or 1648 cm^{-1} (Diller et al., 1987). Band fitting of the hR → hL FTIR difference spectrum between 1655 and 1620 cm^{-1}, to three Gaussian bands, demonstrated a counterion dependence for the positive C=N band due to hL as well as for the negative C=N band due to hR (Table 1). The best-fit position of the C=N positive band in the hR → hL difference spectra ranged from 1642.3 cm^{-1} in Cl^- to 1638.6 cm^{-1} in I^-. Thus, a similar counterion

dependence appears to be associated with the C=N stretching vibration in the hL state as in the hR state.

C=ND Vibrational Frequencies. Figure 1B shows hR → hL spectra of samples in the presence of deuterated buffer containing Cl^- or Br^-; I^- data were not obtained. Deuteration shifts vibrational frequencies of groups with exchangeable protons, including the retinal PSB. The negative band due to the C=N stretch in the hR state downshifts by 10–12 cm^{-1} to ~1620 cm^{-1}, in agreement with prior results (Maeda et al., 1985; Fodor et al., 1987; Diller et al., 1987). Additionally, a new positive band appears in the deuterated hR → hL spectra near 1570 cm^{-1}. This may be attributable to a deuterated arginine side chain, as discussed elsewhere (Braiman et al., 1994).

It is noteworthy that the $Cl^- > Br^-$ ordering of the negative C=N and C=C vibrations that was seen in the undeuterated samples is not observed after deuteration (Figure 1B). If anything, the opposite ordering is observed in the C=N region; however, the small (1 cm^{-1}) apparent upshift between the weak C=ND band in Cl^- and Br^- (Figure 1B) is less significant than the opposite shift of the stronger C=NH bands (Figure 1A). The low intensity of the $C=ND^+$ stretching difference bands (Figure 1B), compared to the $C=NH^+$ bands (Figure 1A), is likely due to greater frequency overlap in the hR and hL states. The $C=ND^+$ stretching vibrations of these photointermediates are at 1620 and 1621 cm^{-1}, as shown earlier by resonance Raman (Fodor et al., 1987; Diller et al., 1987). In FTIR difference spectra (Figure 1B), the overlap leads to nearly complete cancellation of intensities and makes it more difficult to interpret any observed counterion dependence. By comparison, the $C=NH^+$ bands of hR and hL (Figure 1A) are much more separated, giving more easily interpreted difference peaks.

Anion Dependence of the C=N Vibrational Frequency in Model Compound PSBs. Previously, it was shown using solid-state NMR spectroscopy of NRBA salts that the hydrogen-bond strength decreased over the anion series (Cl^-, Br^-, I^-) (de Groot et al., 1989). However, interpretation of spectra of organic crystals can be complicated due to the possibility for multiple interactions between closely packed cations and anions. Dissolving these salts in so-called nonleveling solvents such as $CHCl_3$ is more likely to produce isolated ion pairs, in which a specific stoichiometric interaction between anion and Schiff base is maintained while other interactions are largely eliminated due to solvation (Baasov et al., 1987).

Figure 2 shows the FTIR spectra in the PSB (C=N) and ethylenic (C=C) stretching regions for halide salts of the model compound *N*-retinylidene-*n*-butylammonium (NRBA) in $CHCl_3$. The C=N stretching frequency of the chloride salt is measured to be 1652 cm^{-1}, exactly the same as determined previously by Baasov et al. (Baasov et al., 1987). However, these authors did not present spectra on the corresponding Br^- and I^- salts. On the basis of our new data in Figure 2, the halide dependence of the $C=NH^+$ stretch for NRBA in $CHCl_3$ is roughly 3 times larger than that seen for hR, with 3 cm^{-1} separating Cl^- and Br^- salts and an additional 5 cm^{-1} separating Br^- and I^- salts.

Halide Perturbations of Visible Absorption in hR. The hR visible spectra presented in Figure 3 demonstrate that changes in external halide ions also affect the visible absorption of hR. The shifts observed for hR in the presence of the three halides F^-, Cl^-, and Br^- are generally analogous to those seen previously for the model compound NRBA in $CHCl_3$ and for the three variant forms of bR that lack the normal Asp-85 counterion (Table 2). The bR variants include two mutants

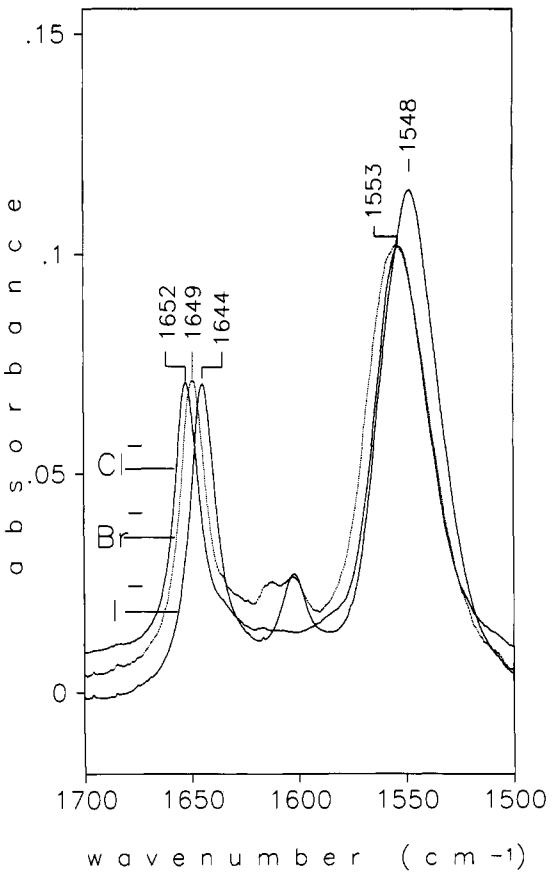

FIGURE 2: Halide-dependent shifts of C=N and C=C vibrational frequencies in FTIR spectra of *N*-retinylidene-*n*-butylammonium (NRBA) salts in $CHCl_3$ solution. An unprotonated Schiff base was first prepared from *all-trans*-retinal and *n*-butylamine dissolved in dry ether. After the ether and excess butylamine were removed by evaporation, the Schiff base was dissolved in cold pentane. Addition of HCl-, HBr-, or HI-saturated cold pentane to separate aliquots of the Schiff base solution caused the corresponding NRBA salts to precipitate. After being washed with cold pentane, these PSB salts were dissolved in chloroform at a concentration of ~10 mM for IR measurements in transmission mode (0.1-mm path length).

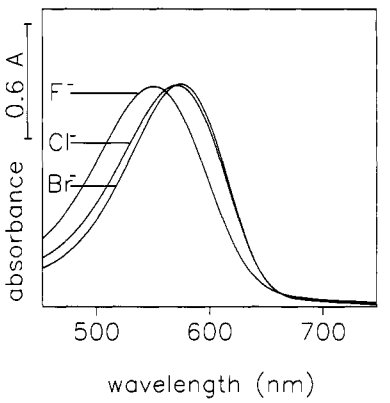

FIGURE 3: Halide-dependent shifts of the visible absorption maximum of hR. Spectra were measured at 0.1-nm resolution on a Shimadzu UV265 double-beam spectrophotometer on samples containing 3 M KF, KCl, or KBr, containing also 0.01% lauryl maltoside and 25 mM MES, pH 6.2. Peaks were normalized to give the same maximum absorbance. The values of λ_{max}, as determined by curve fitting to a Gaussian band shape, are given in Table 2.

in which this residue (along with Asp-212) is mutated to a neutral asparagine. A third bR variant is the low-pH form of wild-type bR, in which Asp-85 is neutralized by protonation. One observation was somewhat anomalous. The visible absorption maximum of hR in lauryl maltoside buffer

Table 2: Halide-Dependent Shifts in λ_{max} of hR and Other Retinylidene PSB Chromophores

halide	hR[a]	$bR_{D85N/D212N}$[b]	$bR_{R82Q/D85N/D212N}$[b]	bR_{acid}[c]	NRBA in $CHCl_3$[d]
F^-	552	556	549	545	468
Cl^-	572	565	563	565	460
Br^-	575	574	573	570	468
I^-	571	580	580	580	478

[a] Solubilized in lauryl maltoside. Measured as described in the Experimental Procedure. [b] A bR mutant lacking an internal PSB counterion. λ_{max} values are reported by Marti et al. (1992). [c] The acid purple form of bR, as reported by Fischer & Oesterhelt (1979). [d] As reported by Blatz et al. (1972). The F^- salt was not the monofluoride.

containing I^- was measured at 571 nm (Table 2; spectrum not shown), 1 nm blue-shifted from the value in Cl^-. This is in contrast to the visible spectra of the other examples in Table 2, for which the maximum in I^- buffer is 6–8 nm red-shifted from its position in Br^- buffer. However, the anomalous hR·I^- result could reflect a partially denatured protein state induced by the combination of detergent and a very large halide ion. The monotonic dependence of $\nu_{C=C}$ with halide-ion size in the detergent-free FTIR samples (Figure 1A), along with the well-established linear correlation of $\nu_{C=C}$ with λ_{max} in retinylidene PSB chromophores (Aton et al., 1977), suggests that in the absence of detergent the λ_{max} dependence would also be monotonic. Light scattering and sedimentation problems prevented us from measuring absorption spectra of detergent-free hR samples with accuracy adequate to test this hypothesis.

With regard to the correlation between $\nu_{C=C}$ and λ_{max}, it is noteworthy that the small $Cl^- \rightarrow Br^-$ red shift of 3 nm in hR (Figure 3 and Table 2) is completely consistent with the observed 1-cm^{-1} downshift of the C=C stretching frequency (Figure 1). This demonstrates that both observed shifts are authentic.

Kinetic FTIR Analysis of the hL → hR Decay at Room Temperature. Time-resolved IR difference spectra have the potential of providing a more reliable view of the hR → hL photoreaction under physiological conditions than do those obtained by low-temperature static difference spectroscopy. We first measured the lifetime of the hL state using 240-μs time-resolved spectroscopy, combined with the statistical technique of singular value decomposition (SVD). Because the SVD analysis was sensitive to statistically correlated changes over the entire 1900–1000-cm^{-1} spectral range, estimation of the number of biochemical decay processes occurring and their time constants by this technique is more reliable than estimation using single-wavelength methods.

SVD can be viewed as a process of calculating the best approximation (in a least-squares sense) to a measured data matrix while reducing its rank. In this case, the matrix is $\delta\mathbf{A}$, the measured absorbance change at $m = 450$ spectral frequencies and $n = 48$ times after photolysis. If $\delta\mathbf{A}$ could be measured in a noise-free fashion, its rank would be equal to the number of distinct hR photointermediates that are present in the time range of measurement. However, the noise present in the measured $\delta\mathbf{A}$ increases its rank to $n = 48$.

The first-order SVD approximation of $\delta\mathbf{A}$ reduces its rank to 1. This approximation is given by $\delta\mathbf{A} \simeq \mathbf{U}_1 S_1 \mathbf{V}_1^T$, where $\mathbf{U}_1$ and $\mathbf{V}_1$ are normalized column vectors with m and n elements, respectively, and the multiplicative constant S_1 is termed the first singular value. The $m + n + 1$ elements of $\mathbf{U}_1$, S_1, and $\mathbf{V}_1^T$ are defined uniquely by the condition that their product gives the minimum possible least-squares deviation from the original measured $m \times n$ matrix $\delta\mathbf{A}$.

The second-order SVD can be described as the first-order SVD term given above plus a second-order term, $\mathbf{U}_2 S_2 \mathbf{V}_2^T$. The normalized column vectors $\mathbf{U}_2$ and $\mathbf{V}_2$ are dimensioned

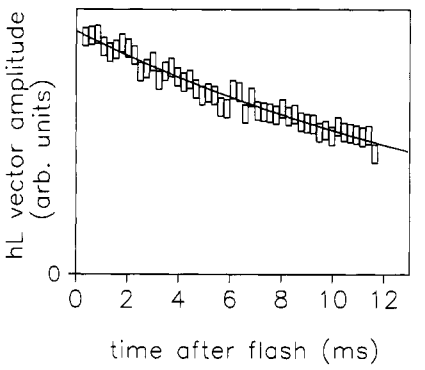

FIGURE 4: Time course of the hL → hR decay at 20 °C, measured in saturated KCl, pH 7.2, 25 °C, as determined from TR-FTIR difference spectroscopy. The plot represents $\mathbf{V}_1^T$, the time-course row vector which, when multiplied by a singular value (a scalar quantity, S_1) and the first basis spectrum column vector ($\mathbf{U}_1$), regenerates the closest approximation to the original absorbance-change data matrix. (See text for further details for the definition of $\mathbf{U}_1$ and $\mathbf{V}_1$). This original data matrix consisted of FTIR difference spectra measured at 2-cm^{-1} intervals (4-cm^{-1} spectral resolution) and at 48 different times following the 530-nm photolysis flash. During each 240-μs time interval, 16 interferogram points were digitized. The plotted $\mathbf{V}_1$ was calculated by means of a computerized singular value decomposition algorithm as described by Chen & Braiman (1991). It represents the most significant time course (or vector amplitude) of intensity changes occurring in a correlated fashion throughout the 1900–1000-cm^{-1} spectral range. On the basis of previously published descriptions of the hR photocycle (e.g., Zimányi & Lanyi, 1989), this first time course is associated with the hL → hR decay process. The best-fit single-exponential decay curve is shown superimposed on the 48 individual time points. The optimized time constant was 19.1 ● 0.8 ms.

as before, and S_2 is termed the second singular value. Again, S_2, $\mathbf{U}_2$, and $\mathbf{V}_2$ are determined uniquely by the requirement of providing the best least-squares fit to the original data matrix, along with the condition that $\mathbf{U}_2$ must be orthogonal to $\mathbf{U}_1$ and $\mathbf{V}_2$ must be orthogonal to $\mathbf{V}_1$. The SVD process can be continued until the total number of terms is equal to the rank of the original matrix $\delta\mathbf{A}$. However, the singular values eventually drop to a level indicative of the measurement noise, at which point the SVD can be truncated without losing any useful information.

In the SVD spectral analysis here, $\mathbf{U}_i$ and $\mathbf{V}_i$ are referred to as basis spectra and time courses, respectively. The plot of $\mathbf{V}_1$ in Figure 4 thus represents the time course of the most statistically significant correlated decay process occurring over the period being analyzed, which ran from 0.244–12 ms after photolysis. (Digitized data measured from 0–0.244 ms were not included in the statistical analysis due to the presence of a 530-nm photolysis flash artifact picked up by the IR detector). The singular value S_1 corresponding to this time course is nearly an order of magnitude higher than the next highest singular value S_2 (5×10^{-4} compared to 8×10^{-5}). This indicates that to a good approximation, all of the measured absorbance changes can be accounted for by the first-order SVD, that is, the measured absorbance changes generally

correspond to the appearance and decay of a single photointermediate, hL. This means furthermore that to a close approximation, the basis spectrum U_1 must correspond to a normalized hR → hL difference spectrum. The second most significant time course V_2 probably contained a small amount of useful information about the hL → hO process, since just above the noise it showed one (faster) apparent decay constant in addition to that seen in the first time course; the corresponding basis spectrum U_2 had features that could be attributable to the hO vibrational spectrum, e.g., a strong difference peak near 1500 cm^{-1} (data not shown).

SVD is particularly useful for determining time constants more accurately than is possible with single-wavenumber kinetic analysis. This is because the time courses determined from SVD exhibit exponential decay constants identical to those corresponding individual wavenumber positions but with much better signal/noise ratios. The first time course V_1 was fit by computer (using Matlab software) to a single exponential with a time constant of 19.1 ± 0.8 ms (solid curve in Figure 4). Fitting of this time course to an additional time constant, or to an additional constant base-line offset, decreased the variance of the 48-point fit by <5%. This confirms that the first basis spectrum U_1, obtained by SVD of a data matrix measured in the mid-IR spectral range between 0.244 and 5.5 ms after photoinitiation at room temperature, will correspond principally to the difference spectrum of hR with its photoproduct hL (or with hL and other photointermediates in a fast equilibrium), decaying via a single-exponential process.

Time-resolved visible absorption spectroscopy has been used previously to determine the following room temperature rate constants for the kinetic model below: $k_1 = 210\ s^{-1}$; $k_2 = 470\ M^{-1}\cdot s^{-1}$; $k_3 = 310\ s^{-1}$ (Lanyi & Vodyanoy, 1986).

$$hL\cdot Cl^- \underset{k_2}{\overset{k_1}{\rightleftharpoons}} hO + Cl^- \xrightarrow{k_3} hR\cdot Cl^- \qquad (1)$$

Under our measuring conditions of high KCl concentration (estimated to be near saturation, or ~4.5 M), the equilibrium between hL and hO is calculated to be fast and to favor hL. To a good approximation, then, the only apparent rate constant that one expects to observe is $k_{app} = (k_1k_3)/(k_2[Cl^-]) = 31\ s^{-1}$. An identical value of k_{app} can be calculated from resonance Raman data (Ames et al., 1992). This value for k_{app} is also fairly close to the fitted decay constant of 52 s^{-1} in Figure 4. The discrepancy could be due to an error in the estimated concentration (or, more to the point, the estimated activity) of Cl^- in our sample, which had much higher concentrations of both protein and KCl than were examined in the cited visible and Raman measurements.

Our kinetic FTIR results are thus completely consistent with the earlier visible and Raman data. All indicate that under high salt conditions, the main event occurring on the 1–10-ms time scale is the decay of the hL_{520} intermediate back to the starting state, hR_{578}, and the only photointermediates ever present in significant concentrations after 0.2 ms are hR and hL.

Comparison of Low-Temperature and 5-ms Time-Resolved Measurements of the hR → hL FTIR Difference Spectrum. Samples of hR, especially those containing I^-, were found to photobleach irreversibly over the course of several thousand flashes. This prevented the collection of high signal/noise TR-FTIR difference spectra with 2-cm^{-1} spectral resolution and 0.24-ms temporal resolution. However, under conditions such as those prevailing in our FTIR samples at room temperature, where the decay of a single photointermediate back to its starting state predominates on the microsecond time scale, stroboscopic FTIR difference spectra with 5-ms time resolution are expected to represent essentially pure difference spectra between two states (Braiman et al., 1987). We took advantage of this fact and used a slower (5 ms) temporal resolution to speed up the process for obtaining hR → hL difference spectra at room temperature with 2-cm^{-1} resolution (Figure 5).

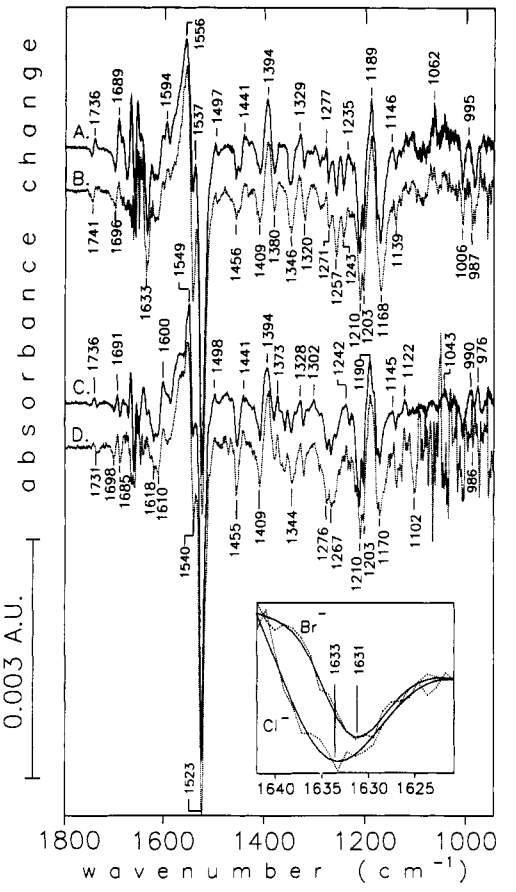

FIGURE 5: Comparison of low-temperature and time-resolved FTIR difference spectra of the hR → hL photoreaction, in normal (A, B) and D_2O-exchanged (C, D) samples. A and C (solid lines) are static difference spectra measured at 250 K in KCl-saturated H_2O or D_2O, respectively, at 1-cm^{-1} resolution. A is the average of absorbance difference spectra calculated from a series of 276 single-beam intensity spectra taken alternately with the actinic light on and off. Each of these 276 spectra was obtained using 250 interferometer mirror scans, or 3.5 min of measurement time. C is the average of absorbance difference spectra calculated from 206 single-beam intensity spectra measured as in A, except that each of these 206 spectra represented 500 coadded interferorams, i.e., light-on and light-off conditions were maintained for 7 min at a time. B and D (dotted lines) are 5-ms time-resolved difference spectra obtained with 2-cm^{-1} resolution at 20 °C in the same sample buffers as A and C, respectively. Each is based on data taken after ~1.7×10^5 photolysis flashes. Positive (hL) peaks are labeled at precisely correct frequencies for the low-temperature spectra and negative (hR) peaks for the time-resolved spectra. Inset: an expansion of the C=NH stretching region of the 5-ms time-resolved FTIR difference spectra (dotted lines). These spectra were both taken with the sample at 20 °C, in saturated KCl or KBr, as indicated, in undeuterated (H_2O) buffer, and at 2-cm^{-1} resolution. Superimposed on each is the best-fit skewed Gaussian curve (solid lines).

The slower time resolution is expected to introduce some errors relative to the 0.244-ms time-resolved technique. This is principally because the hL concentration decays by ~23% over the course of each 5-ms interval during which a 512-point segment of the difference interferogram is digitized. The effect of this decay on the final hR → hL spectrum is

nevertheless expected to be rather small. The measured 5-ms difference interferogram should be equal to the "true" difference interferogram (i.e., the one that would be measured by sampling a single time point ~1 ms after each flash and taking several thousand flashes to build up a single interferogram) multiplied by a function that approximates a sawtooth with a nonzero base line. After apodization and Fourier transforming this product, each "true" spectral peak is expected to be broadened by convolution with a band-shape function that is the Fourier transform of the sawtooth with nonzero base line. The nonzero constant base line, which is 3 times the maximum value of the varying component, Fourier transforms to a δ-function, guaranteeing that about 75% of each spectral band's intensity is completely unbroadened.

The ~25% sawtooth is expected to contribute, on top of the central δ-function in the band shape, a series of progressively smaller sidebands. These sidebands should be at spacings equal to the reciprocal of 0.065 cm (the interferometer retardation change that occurs during 5 ms), or every 15 cm^{-1}. Such sidebands were not detectable above the noise in the 5-ms TR-FTIR difference spectra of the hR → hL photoreaction at room temperature (Figure 5). These, in fact, appear remarkably similar to 250-K static difference spectra, for both undeuterated (top) and deuterated (bottom) buffers containing Cl^-.

The inset to Figure 5 shows an enlargement of the chloride time-resolved spectrum in the C=N stretching region along with a corresponding bromide time-resolved spectrum. These data demonstrate that even with somewhat poorer spectral resolution, the time-resolved technique can detect an external halide-ion dependence for the Schiff base $C=NH^+$ stretch similar to that seen for the low-temperature case. It was not possible to obtain a comparable time-resolved spectrum in I^- at 2-cm^{-1} resolution because of faster irreversible photobleaching than with the other halides. However, time-resolved FTIR difference spectra at 4-cm^{-1} resolution (not shown), obtained with considerably fewer photolysis flashes, clearly demonstrated C=N and frequency downshifts between Cl^- and I^- samples that were consistent with those observed in the low-temperature static difference spectra (Figure 1). Thus, time-resolved FTIR difference spectra of the hR → hL photoreaction confirm both the Br^-- and I^--induced downshifts of the hR C=N stretching frequency.

Effects of Nitrate on the hR Photoproduct Difference Spectrum. The 5-ms time-resolved difference spectrum measured in NO_3 with 8-cm^{-1} spectral resolution (Figure 6) demonstrates the presence of multiple starting states as well as multiple photointermediates produced under conditions where normally only hL is seen. These states give rise to additional negative (e.g., 1666, 1539, and 1470 cm^{-1}) and positive (1635 and 1508 cm^{-1}) bands on top of those seen in the presence of the halides (Figures 1 and 5).

DISCUSSION

Previously, conclusions about interactions of anions with the chromophore PSB of hR have depended heavily on comparisons of hR properties measured in the presence of Cl^- to those measured in the presence of polyatomic anions such as NO^-_3 and ClO^-_4. However, relative to Cl^-, polyatomic anions are transported very poorly by hR (Schobert et al., 1986) and are thought to bind differently to the protein (Pande et al., 1989). Even NO^-_3, which is pumped measurably by hR, is thought to produce an equilibrium between two different protein structures upon binding to hR. These conformations are thought to undergo two different photocycles, only one of

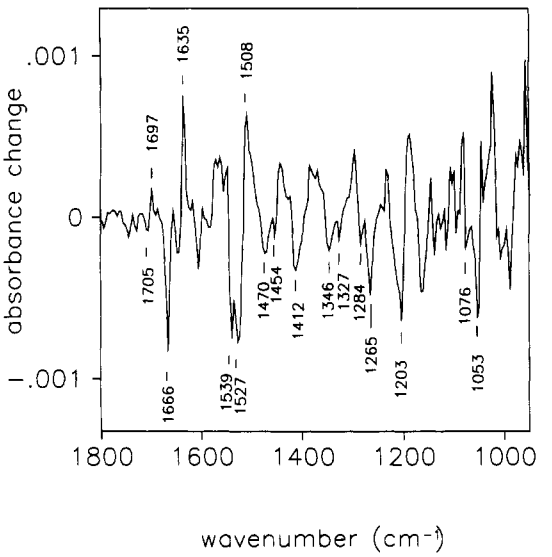

FIGURE 6: Five-microsecond time-resolved FTIR difference spectrum of the hR → hL photoreaction in the presence of saturated KNO_3, no halides, 20 °C. Other conditions were as in the spectra in Figure 5B,D, except that the spectra resolution was 8 cm^{-1} and data were averaged from only ~10^4 photolysis flashes. All labeled peaks were reproducible in a 5-ms time-resolved FTIR difference spectrum obtained under similar conditions, except a lower temperature (10 °C; data not shown).

which resembles the normal hR·Cl^- photocycle (Lanyi, 1990). Our hR → hL spectra measured in the presence of NO^-_3 (Figure 6) strongly support this conclusion. Large spectral perturbations (relative to the same spectrum measured in the presence of Cl^-) include new negative and positive bands. These indicate that not only are different photoproducts produced in the presence of NO^-_3 but also a new starting conformation for the protein and/or chromophore complicates the interpretation of the spectrum.

In contrast, even in the presence of I^-, which is pumped with somewhat less efficiency than Cl^- or Br^- (Schobert et al., 1986), an hR → hL difference spectrum is obtained that is nearly identical to that obtained in the presence of Cl^-. Only a few spectral regions are perturbed, while elsewhere the peak frequencies coincide with great precision. This is true not only between 1650 and 1550 cm^{-1} (Figure 1A) but also over the entire spectral range between 1800 and 1500 cm^{-1} (data not shown). Thus, there is a very clear interpretative advantage in using only halide-series perturbations to analyze anion–protein interactions in hR. The halides produce effects that are large enough to detect with vibrational spectroscopy while minimizing complications due to secondary effects, specifically, the gross conformational and photocycle changes that appear to accompany binding by nitrate and other complex anions.

The FTIR difference spectra in Figure 1 show clearly that the frequency of the C=N stretching vibration of hR is sensitive to which halide is present as a counterion for the PSB. This indicates that the halide ions form direct hydrogen-bonded salt bridges with the retinylidene PSB, as concluded also in a preliminary report of this work (Walter & Braiman, 1992). However, that report examined hR samples in Cl^- and I^- only and at lower spectral resolution than presented here. New TR-FTIR data (e.g., Figure 5 inset) also demonstrate that the anion dependence is detectable at physiological temperatures, indicating that it is not an artifact of low-temperature static difference spectroscopy.

The shifts observed in hR over the series (Cl^-, Br^-, I^-) are about one-third of those seen in $CHCl_3$-dissolved halide salts of model compounds such as NRBA (Figure 2) or unconju-

gated alkylimines (Lussier et al., 1991). This is consistent with a model for the hR Schiff base in which the halide ion is a hydrogen-bond acceptor but not as strong an acceptor as in Schiff base salts dissolved in $CHCl_3$. Instead, in hR, it is likely that one other negatively charged residue (Asp-238) and one or more polar groups (e.g., Tyr-77, water) also participate in hydrogen bonding with the Schiff base group. According to models proposed previously for bR (de Groot et al., 1989; Mathies et al., 1991), formation of such a complex counterion could weaken the hydrogen bonds formed with the PSB.

Halide dependence of hR → hL vibrational difference bands in other spectral regions indicates that an arginine residue, possibly Arg-108, is also involved in hydrogen bonding with chloride (Braiman et al., 1994). Thus, the halide perturbation effects on the hR vibrational spectrum spport a two-anion, two-cation model for the Schiff base binding site in hR. This model is consistent with suggestions by earlier workers (Diller et al., 1987; Dér et al., 1991; Ames et al., 1992) that in hR, externally supplied halide ions substitute for the negatively charged Asp-85 counteranion of bR, for which no hR homolog exists. It is also consistent with the spatial coordinates of the bR homologs of the other residues mentioned above (Asp-212 and Arg-82) in the structural model deduced by Henderson and co-workers from electron microscopy (Henderson et al., 1990).

The fact that halide-dependent perturbations are also seen for the C=NH stretching vibration in the hL state strongly supports the proposal by Ames et al. (1992) that in this state the halide is still bound to the Schiff base. The overall increase in hydrogen-bond strength between hR and hL might reflect a loss of PSB and halide interactions with other components of the PSB binding pocket of hR, specifically Asp-238 and Arg-108. As suggested by Ames et al., the overall function of the chromophore *trans* → *cis* photoisomerization during the hR → hL reaction would then be to carry the halide away from its starting site within the protein to another site where it is more weakly bound and can be lost to the internal medium upon hO formation.

Counterion dependencies in the C=N spectral region of hR have been observed previously using resonance Raman spectroscopy. However, C=N Raman frequency shifts were observed only when spectra obtained in the presence of Cl^- were compared with spectra in the presence of polyatomic anions such as NO^-_3 and ClO^-_4 (Maeda et al., 1985; Pande et al., 1989; Ames et al., 1992). Some of the potential difficulties associated with these comparisons are mentioned above. Early workers interpreted the dialysis of chloride-containing samples against nitrate buffer as resulting in removal of chloride, without nitrate replacement into the same binding site (Maeda et al., 1985). The 7-cm^{-1} upshift of $\nu_{C=N}$ that resulted from such dialysis could not be modeled as resulting from a break of a PSB–Cl^- hydrogen bond. It was therefore concluded that halide binding to hR did not involve direct hydrogen bonding to the PSB. This conclusion was supported by subsequent Raman experiments, in which no significant shift was detected when resonance Raman spectra of hR in Cl^- and Br^- buffers were compared (Pande et al., 1989). The latter results supported a previous proposal that halide binding occurred at a site fairly remote from the Schiff base group but still within the chromophore binding pocket, i.e., site II (see below for further discussion of the two-site model for anion binding).

There are several simple explanations for our detection by FTIR difference spectroscopy of a halide-series shift in $\nu_{C=N}$ that was not seen in resonance Raman spectra. First, the FT-IR difference results were obtained using 4–8 times better spectral resolution, without sacrificing signal/noise ratio. Second, the data were obtained with an FT-IR spectrometer, in which all frequencies are automatically calibrated to a precise standard (the frequency of the He–Ne reference laser) to better than 0.1-cm^{-1} accuracy. The earlier Raman spectra may not have been calibrated with enough precision to detect a 1-cm^{-1} shift. Third, we carefully controlled our reconstitution procedures to insure identical lipid/protein ratios in samples prepared with the three different halides. We found that variations in the lipid/protein ratio in samples not prepared in parallel can shift FTIR difference bands by up to ~1 cm^{-1} (data not shown). Finally, our studies included samples in I^-, which induces a larger shift than Br^- and reinforces the conclusions obtained from it.

It should be noted that it may be difficult to detect iodide-induced shifts in Raman experiments, which have a high visible light flux. As mentioned above, we observed that hR samples in buffers containing I^- undergo irreversible photodestruction under intense visible illumination. This problem was exacerbated at subsaturated salt concentrations, in the presence of detergents, at temperatures above freezing, and under the high-pulsed laser intensity used for time-resolved FTIR experiments. Furthermore, we obtained evidence from visible absorption spectroscopy for conformational instability of hR·I^- in the presence of detergents (either lauryl maltoside or octylglucoside). In order to obtain the Raman spectra in I^- without inducing irreversible photobleaching or conformational instabilities, we expect that it will be necessary to duplicate most of our FTIR sampling conditions, i.e., to use detergent-free KI-saturated buffer and to cool the sample as well as to use near-IR excitation and a spinning Raman cell.

In addition to affecting the C=N frequency, hydrogen bonding at the PSB is expected to be closely correlated with the visible absorption maximum (Rodman Gilson et al., 1988). Experimentally, this correlation has been demonstrated with model compounds (Blatz et al., 1972), with the "acid blue" form of bR (bR_{acid}) (Fischer & Oesterhelt, 1979; Dér et al., 1991), and with bR mutants (D85N/D212N and R82Q/D85N/D212N) in which both aspartate counterions (Asp-85 and Asp-212) have been neutralized by mutation (Marti et al., 1992). In these variant forms of bR, the buffer anion serves as the counterion to the Schiff base because the internal carboxylate which normally functions in this role in wild-type bR is neutralized by titration or mutation. For all these variant forms, there is, in general, a progressive red shift in λ_{max} as the halide-ionic radius increases (Table 2).

The visible absorption spectrum of hR in lauryl maltoside detergent also shows clear shifts in λ_{max} as the external halide is changed (Figure 3). These shifts are for the most part completely analogous to those seen in the bR variant forms lacking an internal counterion. The red shift of λ_{max} with increasing external halide size reflects progressive increases in delocalization of the chromophore's conjugated π-electrons. Since this delocalization decreases the force constants of the conjugated double bonds, it can also be detected in the form of halide-dependent changes in $\nu_{C=C}$ (Figure 1).

In constrast, anion-dependent effects on the C=N frequency are thought to be due at least as much to coupling of this stretch with the in-plane C=N—H bending vibration, which has a force field strongly affected by hydrogen bonding, as to altered C=N force constants (Smith et al., 1985; Rodman Gilson et al., 1988). It is well known that deuteration shifts the bending vibration from near 1350 cm^{-1} to the 970–980-

cm^{-1} range, leading to decreased coupling between the bending vibration and the C=N stretch. A corollary to the preceding statements, that has been supported by extensive experiments on model compounds (Baasov et al., 1987), is that deuteration of a PSB leads to decreased sensitivity of the C=N vibration to hydrogen-bonding changes. At the same time, deuteration is not expected to diminish counterion-dependent shifts of the C=N vibration resulting from alteration of the C=N force constant.

These experimentally derived correlations were the basis for concluding, from the measured resonance Raman frequencies of the C=NH and C=ND vibrations in hL and hR, that hL has the more strongly hydrogen-bonded PSB group (Fodor et al., 1987; Diller et al., 1987). The protonated C=N vibration in hL is 15 cm^{-1} higher than the protonated C=N vibration in hR. In theory, such a shift could arise purely from a change in the C=N stretching force constant. However, this explanation is ruled out by the fact that the deuterated C=N vibration in hL is within 3 cm^{-1} of the corresponding vibration in hR (Diller et al., 1987; Fodor et al., 1987). (The greater similarity of the hR and hL C=N frequencies in the deuterated samples also results in the greater intensity cancellation of these bands seen in Figure 1B as opposed to in Figure 1A.) Thus, the high frequency of the C=N vibration in hL is a reflection of stronger hydrogen bonding in this intermediate than in hR.

A similar argument applies to comparisons of hR in the presence of different halides. Increasing the halide size from Cl^- to Br^- produces a 1-cm^{-1} downshift in the C=NH stretching frequency but no detectable downshift in the C=ND stretch (Figure 1). This tends to rule out effects other than direct hydrogen bonding as an explanation for the halide dependence of the C=NH frequency.

Additional evidence for this interpretation comes from the halide dependence of other PSB vibrational modes, specifically the C=N—D bending vibration. While deuteration leads to a decreased sensitivity of the C=N stretching vibration to hydrogen-bond strength, it also generally leads to greater sensitivity of the in-plane C=N—H bending vibration. For example, the C=N—H in-plane bending vibrations of bR and hR at ~1350 cm^{-1} are less than 2 cm^{-1} apart in frequency, but the C=N—D vibration of bR is at 976 cm^{-1} while that of hR (in Cl^-) is at 970 cm^{-1} (Diller et al., 1987). A more extreme example is provided by a comparison of bR with its K intermediate, which is thought to have an even more weakly hydrogen-bonded Schiff base than hR. K has a C=N—D in-plane bending vibration at 918 cm^{-1}, nearly 60 cm^{-1} below its frequency in bR, but its undeuterated C=N—H in-plane bend is best assigned to a band near 1348 cm^{-1}, a mere 8 cm^{-1} below the C=N—H bend of bR (Braiman, 1986).

Thus, an important question is whether halide substitutions affect the frequency of the C=N—D bending vibration in hR. The inset to Figure 1 demonstrates that there are indeed differences in the 970–980-cm^{-1} spectral region between samples containing Cl^- and Br^-. Unfortunately, spectral assignments in this region are complicated by interference between negative (hR) and positive (hL) bands, both of which appear to be sensitive to halide substitutions. Therefore, no firm conclusions can be drawn yet about the size of any halide-dependent shifts of the C=N—D modes in hR and hL. Resonance Raman spectra should help to sort out C=N—D assignments in hR and hL. Such experiments could also be useful in identifying the Schiff base C=N—H and C=N—D out-of-plane wagging vibrations, which are also expected to be quite sensitive to hydrogen-bond strength (Braiman, 1986).

A One-Site Two-State Model for Halide Binding to hR. The presence of hydrogen-bonding interactions between the halide and the Schiff base requires some modification of the two-site model for anion binding to hR (Lanyi et al., 1990). Rather than distinct binding sites for polyatomic anions and halides, our results indicate that unphotolyzed hR has a single tight binding site. (This conclusion does not contradict the presence of several weaker Cl^- binding sites detected by ^{35}Cl NMR spectroscopy (Falke et al., 1984).) Furthermore, this single tight binding site is located within hydrogen-bonding distance of the PSB.

Proponents of a two-site binding scheme have in the past explicitly considered and rejected the idea of a single site (Lanyi et al., 1990), based in part on Raman results that did not manifest the halide-dependent shift reported here. Additional arguments against a single site were adduced from the absence of expected anion concentration dependence for spectral and kinetic shifts resulting from single-site occupancy. Specifically, increasing the concentration of nitrate (when no other anions are present) shifts the pigment between two forms with different spectral and photocycle properties, but this shift does not obey the hyperbolic dependence on nitrate concentration predicted by single-site binding; in particular, it is not saturable (Zimányi & Lanyi, 1989).

However, such complications in anion binding curves can be made consistent with a single-site model when one considers the possibility that binding of polyatomic anions might not be the direct cause of the observed spectral and photocycle changes but instead might help modulate a protein conformational change that is itself the direct cause. This possibility is strongly suggested by the FTIR difference spectrum of the hR → hL reaction in the presence of NO^-_3 (Figure 6). The large new negative difference band at 1666 cm^{-1}, which is in the amide I frequency region and could signal a change in peptide backbone conformation, is consistent with the presence of a new initial protein state in addition to the conformational state that occurs in the presence of halides.

The foregoing experimental evidence leads us to the following two-state model for anion binding to hR, which is proposed as an alternative to the currently accepted two-site model. State I (the active state of hR) is stable only in the presence of a small monovalent anion bound near the chromophore PSB and is most stable when this anion is spherically symmetric, i.e., a halide (Cl^-, $Br^- > I^-$). These halides exhibit the strongest binding to the site, with $K_d \simeq$ 10 mM (Steiner et al., 1984). In state I, weak hydrogen bonding of the PSB with a complex counterion leads to a low C=NH stretch frequency of ~1630 cm^{-1} and a long λ_{max} of ~580 nm; exact values depend on which halide is present.

Binding of polyatomic anions at the same site is somewhat weaker ($K_d \simeq$ 25 mM for NO^-_3), due to altered directionality of hydrogen-bonding and salt-bridge interactions. Furthermore, these interactions tend to be optimized when the protein residues around the binding site adopt a different conformational state (state II). In this state, chromophore PSB interaction with the normal complex counterion is disrupted. Instead, the external anion functions as an exclusive counterion that is more tightly hydrogen-bonded to the chromophore PSB, leading to a high C=NH stretch frequency of ~1645 cm^{-1} and a short λ_{max} of ~565 nm.

Perchlorate, with its large size and tetrahedral symmetry, cannot be accomodated by the geometric constraints for a complex counterion to form state I, and thereby, it forces all of the protein molecules into state II. However, nitrate's smaller size and more planar geometry can accomodate either

state, so that even at saturating nitrate concentrations where the site is fully occupied, an equilibrium is formed between the two states. In hR from *H. halobium*, this equilibrium consists of nearly equal amounts of states I and II. In hR from *Natronobacterium pharaonis*, however, replacement of Arg-103 with valine alters the intramolecular interactions so as to shift the equilibrium almost completely to state I (Duschl et al., 1990).

The foregoing two-state hypothesis provides the simplest explanation for the observation that binding to sites I and II appears to be mutually exclusive (Lanyi et al., 1990); this condition holds automatically if both sites are the same. The protein can only be in state I or in state II, so that addition of different types of anions leads to reversible shifts between the two conformational states, mimicking a mutual competition reaction.

We have not yet quantitatively tested this two-state hypothesis against many experiments that have ben published on hR, and so, it remains somewhat tentative. One published result that causes immediate concern, however, is the claim that hR absorbs maximally at 565 nm even without any external anions bound at all, i.e., the same as in the presence of complex anions (Steiner et al., 1984). This result seems inconsistent with our two-state, one-site model, in which an external anion is always required to provide charge balance in the PSB binding site.

However, charge balance and a 565-nm absorption maximum might both be maintained in the absence of a bound external anion, simply by shifting Arg-108 away from the chromophore binding pocket and toward the external medium. This motion would be analogous to that proposed for the homologous side chain in bR (Arg-82) in response to protonation of the Schiff base counterion (Asp-85) during the photocycle (Braiman et al., 1988). The electron density map (Henderson et al., 1990) supports the idea that there is some flexibility in the positioning of this arginine. Invoking such a motion to explain the 565-nm absorption maximum of anion-free hR would complicate our two-state model by suggesting that at least one additional conformational state must also be accessible to unphotolyzed hR.

ACKNOWLEDGMENT

We are grateful to Richard Needleman for providing halobacterial strains and to Alexandra L. Klinger for assistance in performing SVD kinetic analyses.

REFERENCES

Ames, J. B., Raap, J., Lugtenburg, J., & Mathies, R. A. (1992) *Biochemistry 31*, 5395–5400.
Aton, B., Doukas, A. G., Callender, R. H., Becher, B., & Ebrey, T. G. (1977) *Biochemistry 16*, 2995–2999.
Baasov, T., Friedman, N., & Sheves, M. (1987) *Biochemistry 26*, 3210–3217.
Blatz, P. E., Mohler, J. H., & Navangul, H. V. (1972) *Biochemistry 11*, 848–855.
Bligh, E. G., & Dyer, W. J. (1959) *Can. J. Biochem. Physiol. 37*, 911–917.
Braiman, M. S. (1986) *Methods Enzymol. 127*, 587–597.
Braiman, M. S., & Mathies, R. A. (1980) *Biochemistry 19*, 5421–5428.
Braiman, M. S., Ahl, P. L., & Rothschild, K. J. (1987) *Proc. Natl. Acad. Sci. U.S.A. 84*, 5221–5225.
Braiman, M. S., Mogi, T., Marti, T., Stern, L. J., Khorana, H. G., & Rothschild, K. J. (1988) *Biochemistry 27*, 8516–8520.
Braiman, M. S., Bousché, O., & Rothschild, K. J. (1991) *Proc. Natl. Acad. Sci. U.S.A. 88*, 2388–2392.
Braiman, M. S., Walter, T. J., & Briercheck, D. M. (1994) *Biochemistry* (paper in this issue).
Chen, W., & Braiman, M. S. (1991) *Photochem. Photobiol. 54*, 905–910.
de Groot, H. J. M., Harbison, G. S., Herzfeld, J., & Griffin, R. G. (1989) *Biochemistry 28*, 3346–3353.
Dér, A., Szaáraz, S., Tóth-Boconádi, R., Tokaji, Zs., Keszthelyi, L., & Stoeckenius, W. (1991) *Proc. Natl. Acad. Sci. U.S.A. 88*, 4751–4755.
Diller, R., Stockburger, M., Oesterhelt, D., & Tittor, J. (1987) *FEBS Lett. 217*, 297–304.
Duschl, A., McCloskey, M. A., & Lanyi, J. K. (1988) *J. Biol. Chem. 263*, 17016–17022.
Duschl, A., Lanyi, J. K., & Zimányi, L. (1990) *J. Biol. Chem. 265*, 1261–1267.
Falke, J. J., Chan, S. I., Steiner, M., Oesterhelt, D., Towner, P., & Lanyi, J. K. (1984) *J. Biol. Chem. 259*, 2185–2189.
Fischer, U., & Oesterhelt, D. (1979) *Biophys. J. 28*, 211–230.
Fodor, S. P. A., Bogomolni, R. A., & Mathies, R. A. (1987) *Biochemistry 26*, 6775–6778.
Henderson, R., Baldwin, J. M., Ceska, T. A., Zemlin, F., Beckmann, E., & Downing, K. H. (1990) *J. Mol. Biol. 213*, 899–929.
Kakitani, H., Kakitani, T., Rodman, H., Honig, B., & Callender, R. (1983) *J. Phys. Chem. 87*, 3620–3628.
Kates, M., Kushwaha, S. C., & Sprott, G. D. (1982) *Methods Enzymol. 88*, 98–111.
Lanyi, J. K. (1990) *Physiol. Rev. 70*, 319–330.
Lanyi, J. K., & Vodyanoy, V. (1986) *Biochemistry 25*, 1465–1470.
Lanyi, J. K., Zimányi, L., Nakanishi, K., Derguini, F., Okabe, M., & Honig, B. (1988) *Biophys. J. 53*, 185–191.
Lanyi, J. K., Duschl, A., Váro, G., & Zimányi, L. (1990) *FEBS Lett. 265*, 1–6.
Maeda, A., Ogurusu, T., Yoshizawa, T., & Kitagawa, T. (1985) *Biochemistry 24*, 2517–2521.
Marti, T., Otto, H., Rösselet, S., Heyn, M. P., & Khorana, H. G. (1992) *J. Biol. Chem. 267*, 16922–16927.
Mathies, R. A., Link, S. W., Ames, J. B., & Pollard, W. T. (1991) *Annu. Rev. Biophys. Biophys. Chem. 20*, 491–518.
Ni, B., Chang, M., Duschl, A., Lanyi, J., & Needleman, R. (1990) *Gene 90*, 169–172.
Oesterhelt, D., & Tittor, J. (1989) *Trends Biochem. Sci. 14*, 57–61.
Pande, C., Lanyi, J. K., & Callender, R. H. (1989) *Biophys. J. 55*, 425–431.
Rodman Gilson, H. S., Honig, B. H., Croteau, A., & Zarrilli, G. (1988) *Biophys. J. 53*, 261–269.
Rothschild, K. J., Bousché, O., Braiman, M. S., Hasselbacher, C. A., & Spudich, J. L. (1988) *Biochemistry 27*, 2420–2424.
Lussier, L., Dion, A., Sandorfy, C., Hoa, L.-T., & Vocelle, D. (1991) *Photochem. Photobiol. 44*, 629–639.
Schobert, B., Lanyi, J. K., & Oesterhelt, D. (1986) *J. Biol. Chem. 261*, 2690–2696.
Smith, S. O., Marvin, M. J., Bogomolni, R. A., & Mathies, R. (1984) *J. Biol. Chem. 259*, 12326–12329.
Smith, S. O., Myers, A. B., Mathies, R. A., Pardoen, J. A., Winkel, C., van den Berg, E. M. M., & Lugtenburg, J. (1985) *Biophys. J. 47*, 653–664.
Steiner, M., Oesterhelt, D., Ariki, M., & Lanyi, J. K. (1984) *J. Biol. Chem. 259*, 2179–2184.
Walter, T. J., & Braiman, M. S. (1992) in *Structures and Functions of Retinal Proteins*, (Rigaud, J., Ed.) Vol. 221, pp 233–236, Colloque INSERM/John Libbey Eurotext: London, Paris.
Zimányi, L., & Lanyi, J. K. (1989) *Biochemistry 28*, 5172–5178.